

X-Ray Observations of Optical/IR-Selected Clusters at $Z > 1$ from the SpARCS Survey

E. Ellingson (U. Colorado), A. Muzzin (Yale U.),
D. Burke (CfA), A. Hicks (MSU),
G. Wilson (UC Riverside), and the SpARCS Team

ABSTRACT

We present Chandra and XMM X-ray detections of two galaxy clusters at $z > 1$ from the SPaRCS cluster survey. This survey is based on a wide-field optical-Spitzer photometric survey using the red-sequence cluster-finding technique, and has currently confirmed a significant sample of high redshift clusters. Here we present preliminary X-ray results for clusters at $z=1.34$ and $z=1.004$. Two SPaRCS clusters at high redshift have also been detected as X-ray sources by others. We compare these four clusters with samples of both X-ray selected clusters and lower-redshift red-sequence-selected clusters from the RCS surveys. We find that the SpARCS technique recovers clusters found using X-ray detection techniques, but that red-sequence-selected clusters are systematically lower-luminosity than X-ray selected clusters of similar richness or temperature. We discuss this difference in the context of biases in both the red-sequence and X-ray selection techniques.

The SPaRCS/GCLASS CLUSTER SAMPLE

Galaxy clusters provide valuable constraints on the structure of both the dark matter and baryonic components of universe, and on cosmological parameters (e.g., Vikhlinin et al, 2009a,b). Clusters at $z > 1$ provide particularly strong constraints on the cosmic evolution of both galaxies and large scale structure; however, only a handful of clusters have been discovered at $z > 1$, mostly via X-ray surveys (e.g., Rosati et al., 1999, Mullis et al., 2005, Bremer, et al., 2006, Stanford et al., 2006, and others). However, larger samples of clusters, found by different methodologies, are greatly needed to broaden our understanding of cluster properties.

The SpARCS survey (SPitzer Adaptation of the Red-Sequence Cluster Survey; Muzzin et al., 2009, Wilson et al. 2009) combines IR observations from the widest area Spitzer IRAC survey with 25 nights of deep z' -band imaging data from CFHT/CTIO, to search for very high redshift clusters via the well-established red-sequence method (Gladders & Yee 2005). With 42 deg², the SpARCS survey has discovered ~ 200 new cluster candidates with masses greater than $\sim 10^{14} M_{Sun}$ at $z > 1$. The GCLASS program targets 10 rich clusters at $z > 1$ for extensive spectroscopy with Gemini. A unique aspect of the SpARCS survey is its close analogy to red-sequence selected cluster surveys at

lower redshift (the 100 deg² RCS-1 and 1000 deg² RCS-2 surveys, which target clusters with $0.2 < z < 1.0$; Gladders & Yee 2005). Here we present preliminary results from X-ray observations of SPaRCS clusters and a comparison with RCS and X-ray selected clusters. Throughout, $H_0=70 \text{ km s}^{-1} \text{ Mpc}^{-1}$, $\Omega_M = 0.3$ and $\Omega_\lambda = 0.7$.

Low X-ray Luminosity Clusters and Optically-selected Samples

It has long been known that optical and X-ray selection methodologies yield very different cluster samples, with optical detection finding many more clusters, as well as clusters with systematically lower X-ray luminosities (e.g., Holden, et al., 1997, Donahue et al., 2001, Gilbank et al., 2004, Popesso et al., 2007, Hicks et al., 2008 and others). Some earlier optically-selected samples were plagued by significant substructure along the entire line of sight; however, the red-sequence method quite effectively limits the range of possible contamination to less than 0.1 around the cluster redshift (depending in detail on the cluster redshift, the filters and techniques used). Close to 90% of two dozen RCS clusters targeted with X-ray telescopes have been detected, confirming that these objects do contain a significant virialized overdensity.

The SPaRCS cluster X-ray detections confirm that these clusters are indeed virialized galaxy clusters and that the SPaRCS technique recovers the clusters that are found via X-ray techniques. However, in combination with the RCS clusters, we find a wide range of X-ray luminosities for a given galaxy overdensity, and the mean of these clusters luminosity is systematically lower than for X-ray selected samples at lower redshift. Here we discuss several reasons for the differences in X-ray and red-sequence-selected samples.

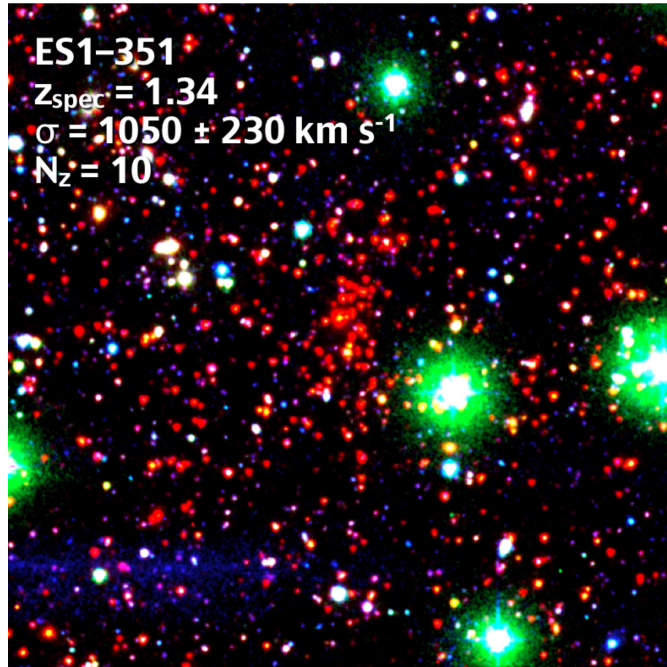


Figure 1: Spitzer/optical images of ES1-351 at $z=1.34$, in the ELAIS south field. The FOV is 5 arcminutes on a side, or ~ 2.5 Mpc at $z\sim 1$.

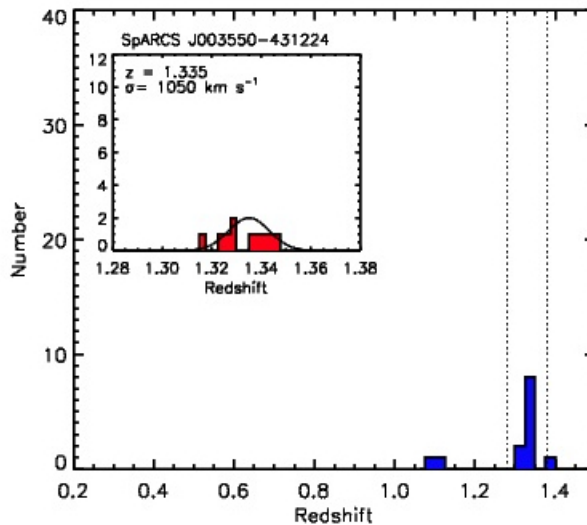


Figure 2: Gemini spectroscopy (see Muzzin et al., 2009; also this conference) identified 10 cluster members for this cluster, and a preliminary velocity dispersion of $1050 \pm 230 \text{ km s}^{-1}$, though this estimate is not yet well-constrained. Additional spectroscopic observations are planned for 2010.

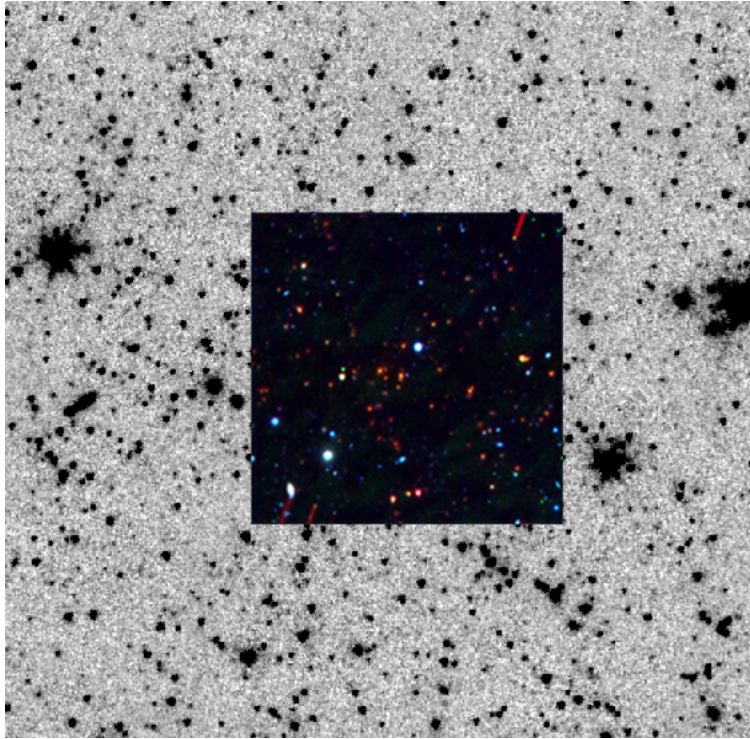


Figure 3: Spitzer/optical images of XMM-129 at $z=1.004$, in the XMM-LSS field. The greyscale image is from Spitzer IRAC, with a FOV of 5 arcminutes on a side, or ~ 2.5 Mpc at $z\sim 1$. The colored offset is constructed from a smaller-FOV K-band image to show the red sequence galaxies in the cluster.

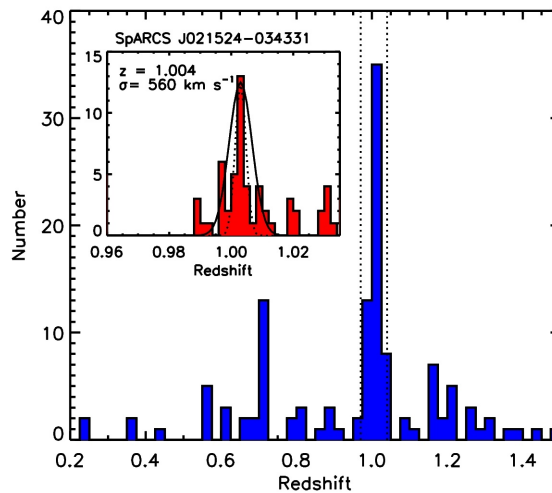


Figure 4: Gemini spectroscopy (see Muzzin et al., 2009; also this conference) identified 48 cluster members for this cluster, and a preliminary velocity dispersion of $560 \pm 60 \text{ km s}^{-1}$, though there may be a dynamically distinct core group with velocity dispersion $\sim 250 \text{ km s}^{-1}$.

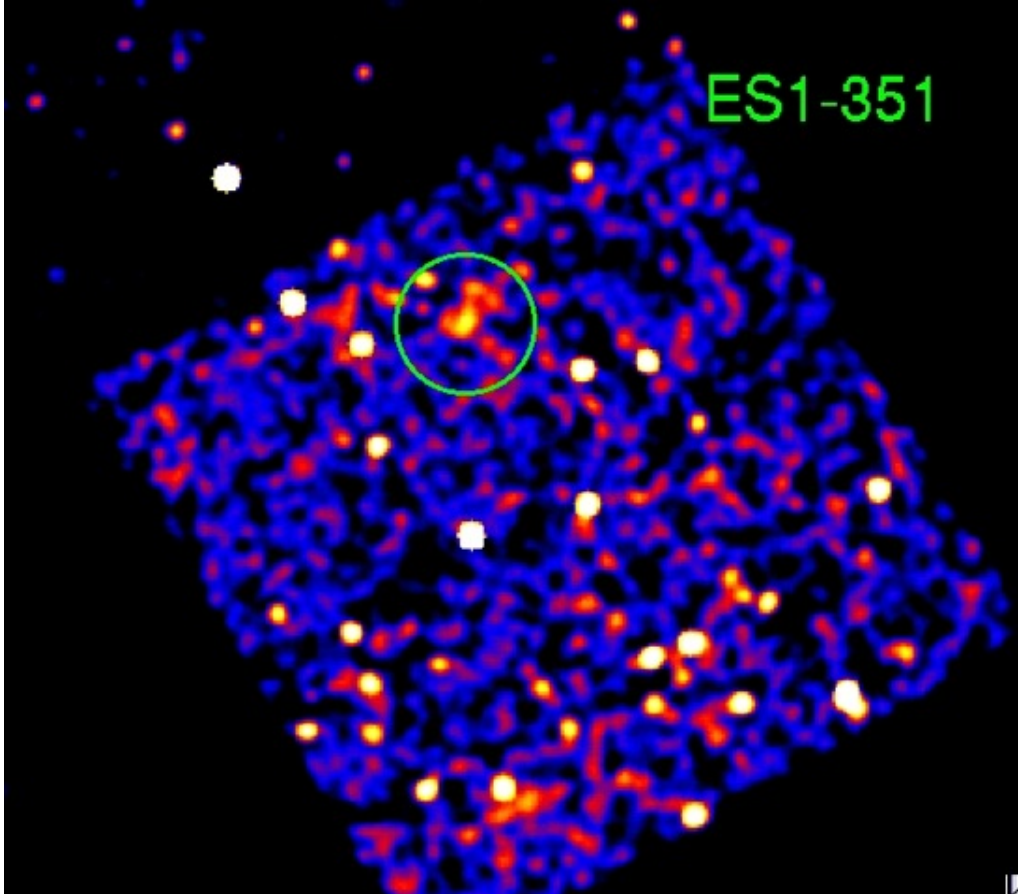


Figure 5: Smoothed Chandra ACIS-S image of ES1-351 in the 0.5-4 keV band. This 63.7 ksec ACIS-S observation was approved for Cycle 11, but was executed in August 2009. The cluster is detected at a significance of about $2.5\text{-}\sigma$, estimated from variations in nearby background regions. The cluster emission is resolved, and the green circle shows a radius of about 50 arcseconds, or 425 kpc at the cluster redshift. The bolometric luminosity of this cluster inside a smaller 220 kpc radius ($\sim R_{2500}$ if $T_X \sim 3$ keV) is estimated to be $0.65 \cdot 10^{44}$ erg s^{-1} . The X-ray emission center is centered 11 arcseconds northwest of the optical/IR centroid and brightest galaxy; this cluster may show evidence of substructure in both the galaxy spatial and velocity distribution (see Figure 1).

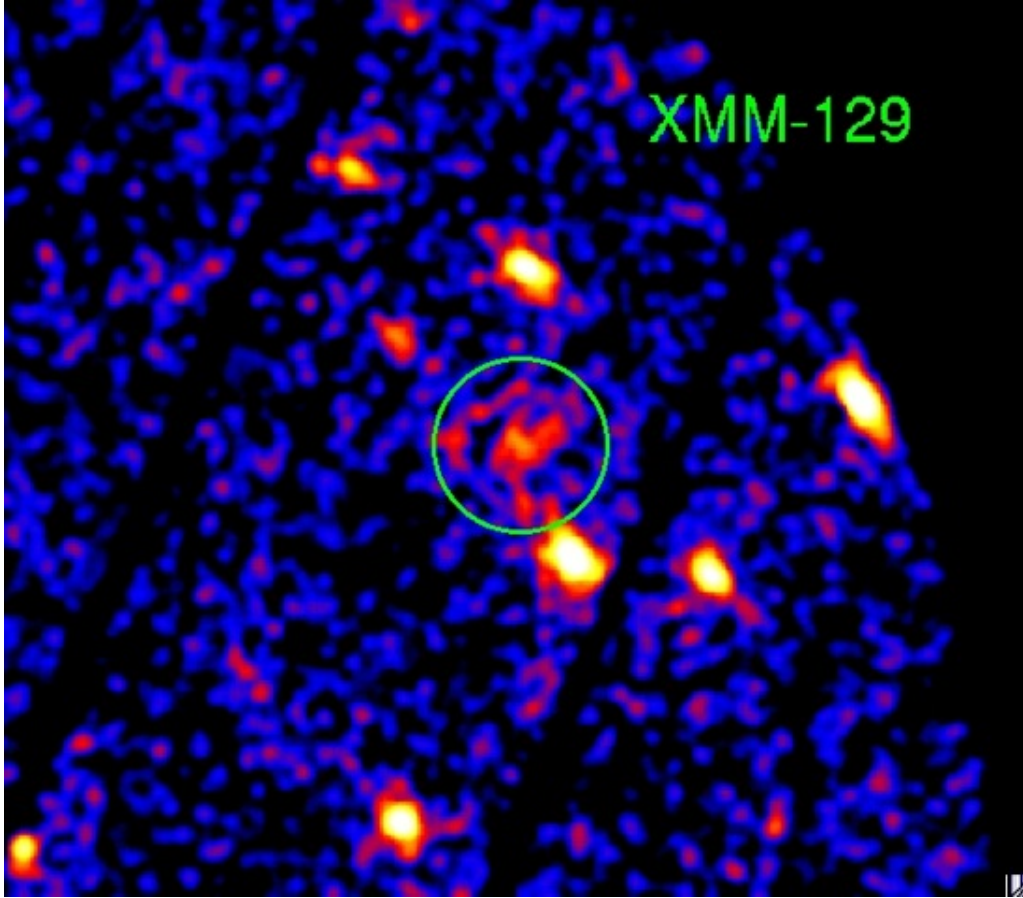


Figure 6: Smoothed XMM image of XMM-129. This 14 ksec observation was taken in January 2007 as part of an extended wide-field survey in the XMM-LSS/SWIRE field by M. Pierre. The cluster is detected nearly exactly on the position of the optical/IR centroid. The other bright objects in the field of view are point sources and likely AGN; the cluster lies significantly far from the detector aimpoint and the PSF is elongated, but the cluster emission is much broader in extent. A second XMM exposure in the same survey also shows a detection of the cluster; however the cluster lies far enough away from the detector center that it is significantly vignetted. The green circle is 400 kpc in size. The luminosity of this cluster inside a 200 radius kpc radius ($\sim R_{2500}$ if $T_X \sim 3$ keV, consistent with the measured velocity dispersion and richness) yields a preliminary estimate of $1.8 \cdot 10^{44}$ erg s^{-1} .

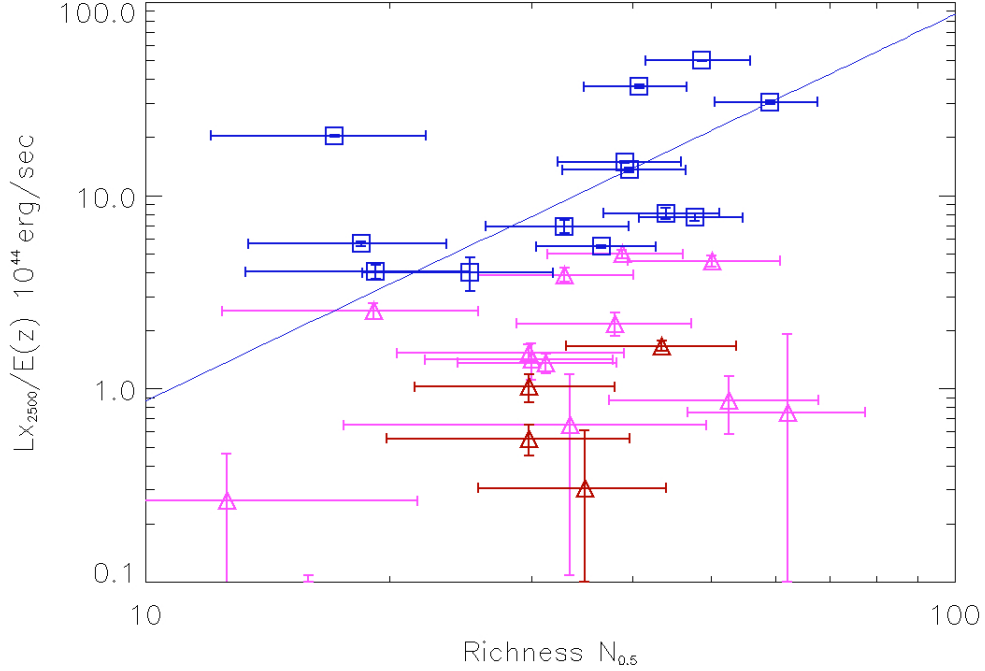


Figure 7: Bolometric X-ray luminosity within R_{2500} versus optical richness for X-ray observations of several samples of galaxy clusters. Blue symbols are from Chandra observations of the massive CNOC X-ray selected clusters, selected primarily from the EMSS X-ray sample, at $0.2 < z < 0.55$ (Yee et al. 1996, Hicks et al. 2006). Pink symbols are Chandra observations of RCS clusters with $0.6 < z < 1.1$, selected from optical surveys for red sequence galaxies (Gladders & Yee, 2005, Hicks et al., 2008). Both of these datasets include corrections for cool cores. Filled red symbols are the two clusters with data presented here. Open red symbols are for two clusters at $z > 1$ in the SPaRCS survey which were previously discovered (Hashimoto, et al., 2002, Bremer, et al., 2006). Our richness parameter is translated from the spatial covariance amplitude, B_{gc} (Muzzin et al., 2007), but here represents the number of red sequence galaxies brighter than $M_* + 1$ within a metric radius of 0.5 Mpc from the cluster core. This parameter is expected to scale as $M^{\gamma/3}$, $T^{\gamma/2}$, or $L^{\gamma/4}$, where the mass density of the cluster is estimated as $\rho \sim r^{-\gamma}$. In the regions measured, $\gamma \sim 2$. (Yee & Ellingson 2003). A best fit to the CNOC data with this power law slope is shown.

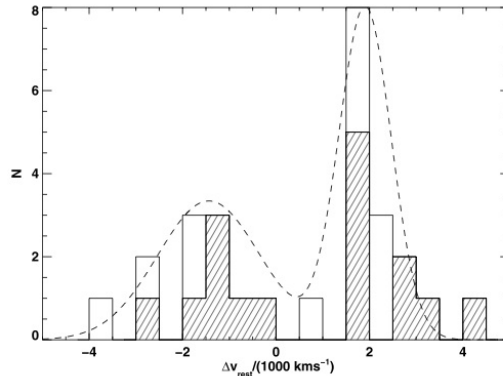


Figure 8: Velocity distribution from galaxies in the low X-ray luminosity cluster RCS043938-29047 at $z=0.96$; this cluster is the rightmost RCS point in Figure 7, and may be similar to ES1-351 . From Cain, et al. 2008.

Geometric Bias and Merging Clusters

Selection using galaxy density projected on the sky necessarily introduces a bias in the types of clusters that are preferred. If all clusters are spherically symmetric, this can be corrected via a conversion from cylindrical to spherical mass, as long as the cluster galaxy density profile is known. However, if clusters are elongated or have correlated structures containing red sequence galaxies, then selection via galaxy overdensity will cause an asymmetric scatter in the masses of clusters at a given measured overdensity. In particular, merging clusters along the line of sight may produce high overdensities and low X-ray luminosities. The most discrepant RCS cluster, RCS043938-29047 at $z=0.96$ was found to be such a system. After detailed spectroscopy, its optical and X-ray properties were successfully modeled as a multi-component system (Gilbank et al. 2007, Cain et al. 2008). This may also be the case for the SPaRCS cluster ES1-351.

Cluster Gas Properties and Selection Bias

While merging clusters and geometric effects can explain some of the highly discrepant clusters found by optical methods, there is evidence that optical richness is a reliable indicator of cluster mass for the bulk of the red-selected samples. Figure 10 shows the temperature-richness relation for RCS and SPaRCS clusters where temperatures are available. Here, red-sequence and X-ray-selected clusters are in agreement within observational scatter. There may be a slight trend for RCS clusters to have higher richnesses at a given temperature, which would most likely indicate a small systematic with redshift in our richness measurement. On this plot, the merging cluster RCS043938-29047 is clearly anomalous.

If richness provides a mass indicator which is reliable for most of the clusters in our sample, then the systematically lower luminosities of the RCS/SPaRCS clusters suggest that the red-sequence technique probes a population of clusters with lower intrinsic luminosities, possibly due to a lower core gas fraction. These could be due to increased AGN activity or cluster mergers, both of which may be more common at higher redshifts. Figure 10 shows the L_X - T_X relation for our samples, showing that they are consistent with a broad range of luminosity for a given temperature, and that the red-sequence selected clusters, which have no selection bias with respect to the cluster gas, are needed to probe the full range of cluster gas properties.

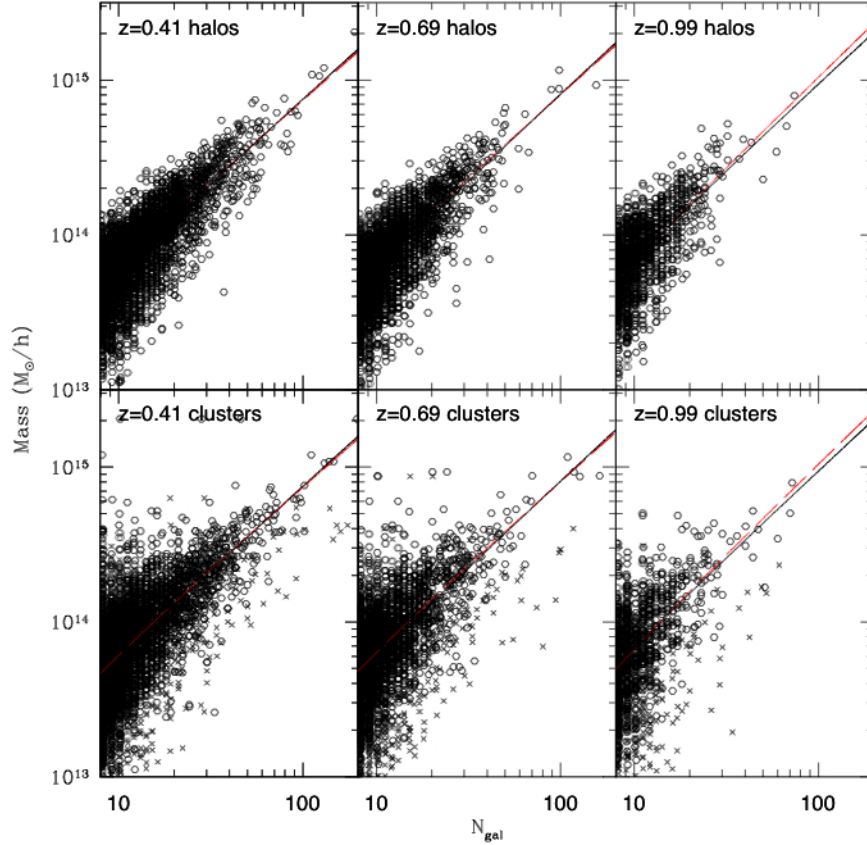


Figure 9: The magnitude of the geometric bias has been estimated via an analysis of the Millennium simulation (Cohn et al. 2007). While the cluster-finding algorithm and richness measurements used for the simulations are not completely analogous, SPaRCS clusters should correspond to about $N > 20$ on the figure above, or masses of $> 10^{14} M_{Sun}$. The top panels (from Cohn et al.) show the halo mass as a function of the intrinsic red sequence galaxy richness; the bottom panels show the largest halo mass as a function of red sequence richness along a single projection. About 10-15% of clusters found by projected galaxy overdensities are comprised of multiple halos, where the mass of the largest halo was less than 50% of the total (tiny crosses). This estimate agrees well with the number of RCS clusters which have X-ray luminosities significantly lower than the expected scalings with richness, or with velocity dispersions which are split into several components (Gilbank et al. 2007, Hicks, et al. 2008, Yan, et al. 2009).

Summary

*We present X-ray detections of two optical/IR-selected clusters at $z > 1$ from the SPaRCS/GCLASS sample, ES-351 at $z=1.34$ and XMM-129 at $z=1.004$. Both clusters were detected as diffuse X-ray sources, indicating that they are virialized overdensities. Adding two clusters which were detected by overlapping X-ray surveys brings the total of high redshift GCLASS clusters confirmed in X-rays to four.

*Comparison of the properties of these clusters with both X-ray and RCS red-sequence-selected clusters confirms the well-established trend that galaxy-selected clusters are systematically lower-luminosity than X-ray selected clusters at a given galaxy overdensity.

*Biases in both the red-sequence and X-ray selection techniques are likely responsible for this discrepancy. Geometric bias arising from counting galaxies on the sky will tend to select systems with associated structure along the line of sight. One very low-luminosity RCS cluster has been identified as a multi-component system, and we suggest that ES1-351 may be similar. Simulations, X-ray and spectroscopic work with the RCS and SPaRCS sample suggest that $\sim 10-15\%$ of red-sequence-selected samples will have measured richnesses that overestimate the main cluster mass by $\sim 50\%$.

* However, for samples with confirmed X-ray temperatures, red-sequence-selected systems still tend to populate the lower-luminosity ranges, suggesting that X-ray selection bias can significantly affect cluster scaling relations, and underscoring the importance of complementary selection techniques for cluster surveys.

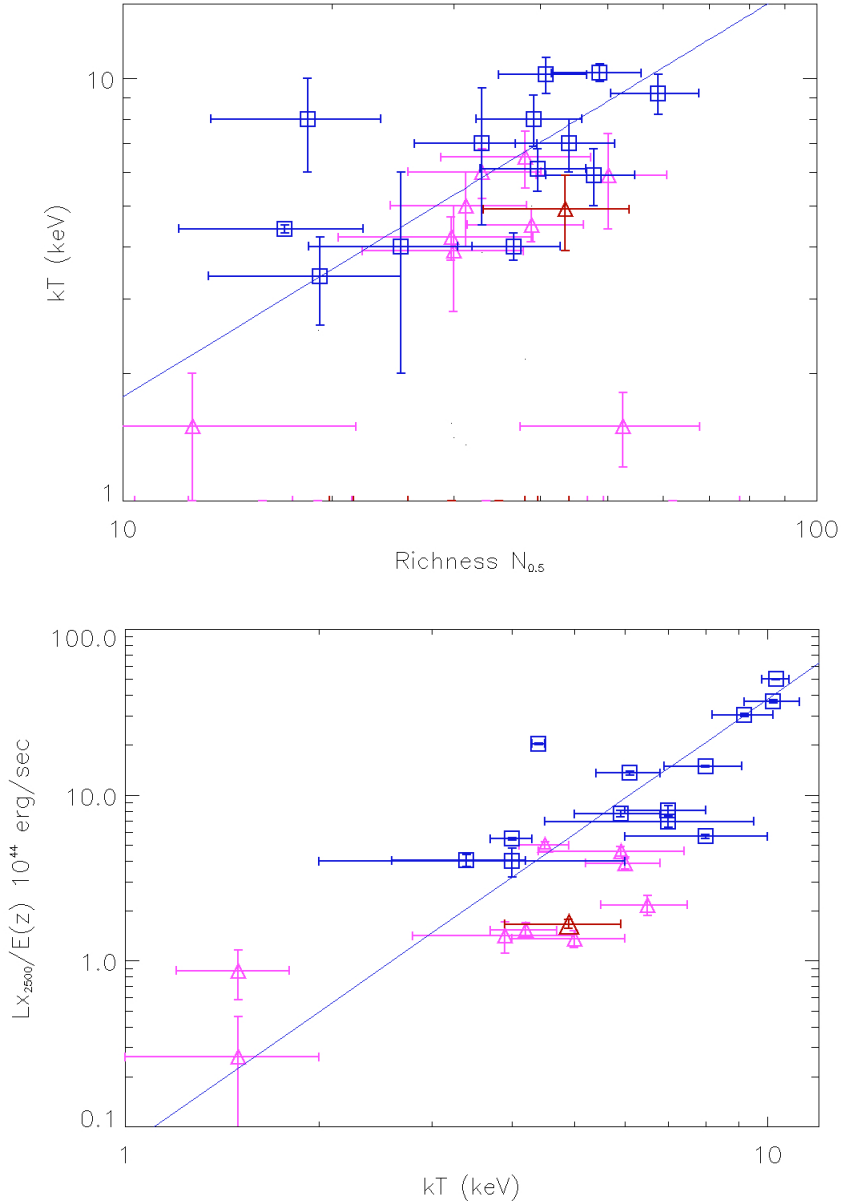


Figure 10: (Top) X-ray temperature versus richness for CNOX X-ray selected clusters (blue), RCS clusters where temperatures could be measured (pink; these omit several of the faintest objects in Figure 7 and thus do not show the clusters that are most discrepant from expected scaling relations), as well as the SPaRCS cluster previously discovered by Hashimoto et al. The line is the best-fit to the CNOX clusters with a power law slope from the expected scaling relation. The highly discrepant point is the merging cluster RCS043938-29047 (see Figure 8). (Bottom) L_X - T_X relations for the same samples. A best-fit line for the CNOX clusters using the scaling relation $L_X \sim T_X^{2.7}$ (Lumb et al. 2004) is shown. RCS/SPaRCS clusters sample the lower- L_X range of the cluster distribution.

References

- Bremer, M., et al, 2006. MNRAS, 371, 1427
Cain, B. et al. 2008, ApJ, 79, 292
Cohn, J., et al, 2007, MNRAS, 382, 1738
Donahue, M. et al., 2001, ApJ 552, 93
Gilbank, D., et al., 2007, AJ, 134, 282
Gilbank, D., et al., 2004, MNRAS 348, 551
Stanford et al., 2006, ApJ, 646, L13
Gladders, M. D., Yee, H. K. C. 2005, ApJS 157 1
Hashimoto, Y., et al., 2002, A&A, 381 841
Hicks, A.K., 2006, ApJ, 652, 232
Hicks, A., et al., 2008, 180, 1022
Holden, B. P., et al., 1997, AJ, 114,1701
Lumb, D.H., et al., 2004 A&A., 420, 853
Mullis et al., et al. 2005, ApJ, 623, L85
Muzzin, A., et al. 2009, arXiv:0810.0005
Popesso, P., 2007 A&A 461, 397
Rosati et al 1999, AJ, 118, 76
Vikhlinin, A, et al. 2009a, 692, 1033
Vikhlinin, A, et al. 2009b, 692, 1060
Wilson, G., et al. 2009, arXiv:0810.0036
Yan, R., et al., 2009, in preparation
Yee, H.K.C., & Ellingson, E., 2003, ApJ, 585, 215